Scanning Electron Microscopy

Volume 1985 | Number 3 Article 17

7-3-1985

Sputter Crater Contour Mapping with Multilayered Films

L. L. Levenson
University of Colorado, Colorado Springs

T. P. Massopust
Solar Energy Research Institute

J. Dick
Solar Energy Research Institute

M. C. Jaehnig
Montana State University

D. Griffith
Hewlett-Packard Corporation

SCANNING ELECTRON MICROSCOPY/1985/III (Pages 1087-1092)
SEM Inc., AMF O'Hare (Chicago), IL 60666-0507 USA

0586-5581/85$1.00+.05

SPUTTER CRATER CONTOUR MAPPING WITH MULTILAYERED FILMS

L. L. Levenson*, T. P. Massopust†, J. Dick†, M. C. Jaehnig**, and D. Griffith††

* Department of Physics and Energy Science
University of Colorado
Colorado Springs, CO 80933-7150

** Center for Research in Surface Science
Department of Physics
Montana State University
Bozeman, MT 59717-0001

† Solar Energy Research Institute
1617 Cole Boulevard
Golden, CO 80401

†† Hewlett-Packard Corporation
1900 Garden of the Gods Road
Colorado Springs, CO 80901-2127

(Paper received February 20, 1985: manuscript received July 03, 1985)

Abstract

Multilayered films composed of alternating 200 Å Al and 267 Å Al_2O_3 layers are made by physical vapor deposition. Twenty-two pairs of these films are deposited on a polished Si wafer. Ion beam sputtering is used to form craters in the multilayered film. When a crater is viewed or photographed *in situ* by scanning electron microscopy, the Al_2O_3 layers appear bright and the Al layers appear dark. In the scanning electron microscope (SEM) the Al_2O_3 layers have a high secondary electron yield compared to Al. In secondary ion mass spectrometry (SIMS), using Cs^+ as the ion beam, imaging with O^- produces an image with Al_2O_3 layers appearing white and with Al layers appearing dark. Scanning Auger microscopy (SAM) imaging of oxygen produces the same result. In all cases, the alternating bright and dark layers along the wall of the sputter crater form a contour map. The width of each bright band represents a change of depth corresponding to the thickness of the Al_2O_3 layer and similarly for the dark Al bands. Therefore, the operator of a SEM, SAM or SIMS unit can determine the depth as well as the shape of a sputter crater *in situ* by using a multilayered film. The main requirement is that the films be smooth on a scale that is small compared to the thickness of each layer and that alternate films have high contrast in the imaging process.

KEY WORDS: Crater imaging, contour mapping, scanning electron microscopy, scanning Auger microscopy, secondary ion mass spectrometry.

*Address for correspondence:
Leonard L. Levenson
Dept of Physics, University of Colorado
Colorado Springs, CO 80933-7150
Phone No. (303) 593-3189

Introduction

Ion beam sputtering is commonly used for in-depth composition analysis with secondary ion mass spectrometry (SIMS), x-ray photoelectron spectroscopy (XPS), Auger Electron Spectroscopy (AES), etc. The depth resolution of a composition profile depends on a number of factors which have been reviewed by several authors[2,4,6,7,10, 12,14-17]. The shape of the ion beam generated sputter crater is the most important instrumental factor[5,6,12]. Static ion beams usually produce shallow ($\lesssim$ 1μm) and broad craters (typically several mm diameter). It is generally assumed that an ion beam has a current density distribution which has a Gaussian function[6,13]. The results of Smith and Walls[13] and Carter et al. [1] indicate that static Gaussian ion beams should produce Gaussian shaped craters. Dynamic rastered Gaussian ion beams can produce broad craters with nearly flat bottoms [13].

An ideal Gaussian crater profiled in the X-direction will have the shape described mathematically by [9]

$$Z = -Zo \exp\left(\frac{-X^2}{2\sigma^2}\right) \qquad (1)$$

where Zo is the maximum crater depth and σ is the crater variance. (For a Gaussian crater, the full width at half maximum (FWHM) = 2.355 σ.) A Gaussian crater formed by a static ion beam during composition profiling would normally have $Zo \ll \sigma$.

The topography of a sputtered crater, produced either by a static or a dynamic ion beam, can be measured by optical interferometry or by means of a mechanical profilometer. However, the crater topography is not easily determined *in situ*. Certainly, the instrument operator can use a variety of calibration materials *in situ* to determine the *outline* of the sputter crater and the *position* of the crater relative to the instrument's detector window. These calibration materials are usually oxide thin films, e.g., Ta_2O_3 on Ta, or SiO_2 on Si. With oxides of known thickness (usually $\sim$ 1000 Å), the sputter rate for the oxide can be measured and a rough outline of the sputter crater can be observed by secondary electron imaging (SEI) in a scanning Auger microscope (SAM), or by secondary ion imaging (SIMS or ISS). An SEI micrograph of a

sputter crater made in a 1000 Å SiO_2 film on Si is shown in Fig. 1. The crater outline is evident, but there is no information about the crater shape or the flatness of the bottom evident in this micrograph.

Zalar and Hofmann [18] have shown that multilayer thin films can be used to image the contour of a crater wall. They used Ni/Cr multilayer thin films. Because of the low electron imaging contrast for a pure element couple such as Ni and Cr [10], Zalar and Hofmann preferred SAM mapping to SEI.

Levenson [8] has used Al/Al_2O_3 multilayered thin films to image the contours of sputter craters in situ with SEI in a SAM instrument. Here, it is shown that contour maps of craters in multilayer thin film sandwiches composed of a metal (Al) and its oxide (Al_2O_3) can be imaged in situ with SEI, SAM or SIMS. Such contour maps allow the experimenter to verify the crater shape as a function of sample position and ion beam parameters.

Experimental

A multilayered film composed of alternating layers of Al and Al_2O_3 was deposited on a polished Si wafer. A smooth substrate is important because Hofmann et al. [4] have shown that substrate surface roughness greatly influences interface broadening during sputter etching. The Al and Al_2O_3 were electron beam evaporated in a diffusion pumped, liquid nitrogen trapped stainless steel bell jar. The pressure during evaporation varied over time from about 10^{-4} down to 10^{-5} Pa (the pressure decreasing as the sources were outgassed during evaporation). A water cooled quartz crystal microbalance (QCM), positioned at the same distance from the evaporation sources as the Si wafer, was used to monitor the deposition rate and the total thickness of Al and Al_2O_3. The theoretical bulk densities of Al and Al_2O_3 were used to calculate the film thickness from the QCM frequency shift. A shutter between the evaporation source and the sample and QCM was used to terminate depositions. The main source of uncertainty in film thickness determination was estimated to be the thermal radiation load on the QCM. The thermal radiation caused a small frequency shift during evaporation. This uncertainty for Al and Al_2O_3 thickness was about five percent. The Al was evaporated from a graphite crucible and the Al_2O_3 was evaporated from a water cooled copper crucible. An e-beam at 5 kV was used to evaporate each material. The Al and Al_2O_3 films were nominally 200 Å and 267 Å thick, respectively. The multilayered sandwich used for this study consisted of twenty-two pairs of films with the outer film composed of aluminum.

If an ideal Gaussian crater is sputter etched in a multilayered sandwich composed of 200 Å Al and 267 Å Al_2O_3 films, the projection of the layers onto a plane would appear as in Fig. 2. For purposes of illustration the vertical and horizontal scales differ appreciably.(Horizontal scale/vertical scale=2000.)

A static Ar^+ ion beam at 700 eV and 370 $\mu A/cm^2$ was impinged onto the Al/Al_2O_3 multilayer film in a Physical Electronics Industries Model 595 Multiprobe. After 18 min. of sputter time, a SEM micrograph of the crater was made. The result is shown in Fig. 3. The alternating light and dark rings originate from the exposed Al_2O_3 and Al layers which line the crater surface. The crater is obviously more asymmetric in the vertical direction than in the horizontal direction. This asymmetry originates in the ion beam direction (45^o) relative to the sample normal. The spacing of the rings approximates the spacing expected for a distorted Gaussian crater.

Assuming that the inner light spot in Fig. 3 indicates that the lowest aluminum film has barely exposed the Al_2O_3 film below it, we take the elevation change from the center of the light spot to the outer edge of the first dark ring to be approximately 200 Å. The distance from the inner edge of the first bright ring to its outer edge represents an elevation change of approximately 267 Å, and so on. If we divide the distance from the center of the inner spot to the edge of any ring by the magnification of the micrograph (32X on the original), we obtain the distance X from the Z axis to the crater surface. A plot of X vs. Z along the horizontal line through the center spot in Fig. 3 is given in Fig. 4. Here, "left" and "right" refer to directions relative to the central spot in Fig. 3. The cross-section shown in Fig. 4 approximates a Gaussian shape within 0.8 mm of the crater center (in the horizontal direction).

Fig. 5 is a secondary electron detector (SED) image of the edge of a crater formed in the same Al/Al_2O_3 multilayered sandwich described above. Here an Ar^+ ion beam at 5 kV, 340 $\mu A\ cm^{-2}$ was rastered over 3 x 3 mm for 72 min. The sample holder was a 60^o fixture in a Physical Electronics Model 595 Multiprobe. While the crater center is relatively flat, the crater edge is quite steep, as shown by the closeness of the contour lines. The crater center is located at the lower left edge.

Auger mapping of sputter craters in multilayered films composed of Al and Al_2O_3 can be carried out with the Al KLL Auger transition. The energy difference between the Al KLL emission (68 eV) from Al and Al_2O_3 (51 eV) is well known [3]. Fig. 6 is an Al KLL Auger electron map of the same area shown in Fig. 5.

Multilayered films can be used to produce contour maps of the craters generated by ion beam bombardment as for SIMS and ion milling. An unrastered, focused ion beam impinging on a solid surface will produce a sputter crater having dimensions representing ion beam density. An example of this effect has been produced using the Cameca ims-3f SIMS instrument. The Al/Al_2O_3 multilayer film previously described was struck by a 35 nA, mass analyzed Cs^+ ion beam. The sample, held at -4500 V, was hit by the beam at an angle 30^o from the normal. Figure 7 shows the result of sputtering with the beam in a spot mode for a few seconds before applying a broad raster (500 x 500 μm) to amply retard the erosion rate while imaging $^{16}O^-$ across a 400 x 400 μm area of the surface.

The triangle roughly defined by the outer

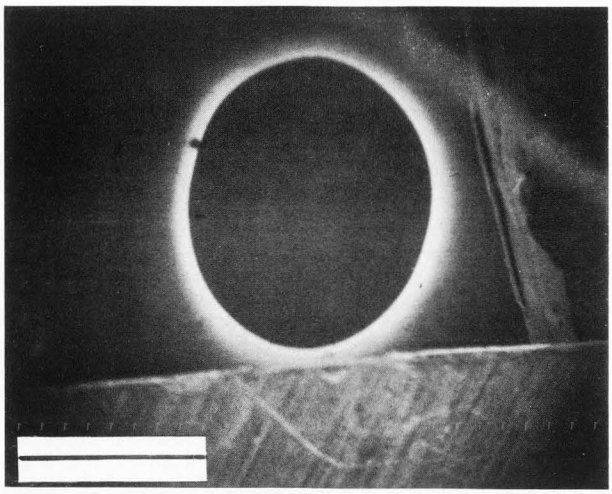

Fig. 1. Secondary electron image of a sputter crater etched in a 1000 Å SiO_2 film on a Si substrate. The argon ion beam current was 370 $\mu A\ cm^{-2}$ at 1.5 keV. The beam rastered over 1x1 mm. The ion beam direction was 45° from the sample normal. Bar = 1 mm.

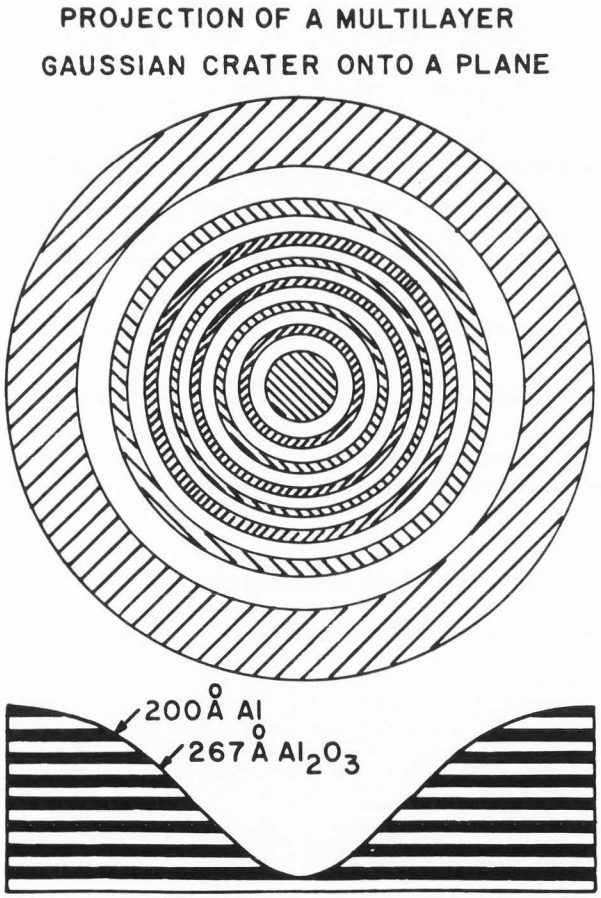

Fig. 2. A contour map of an ideal Gaussian crater in a multilayered film composed of 200 Å Al and 267 Å Al_2O_3 films.

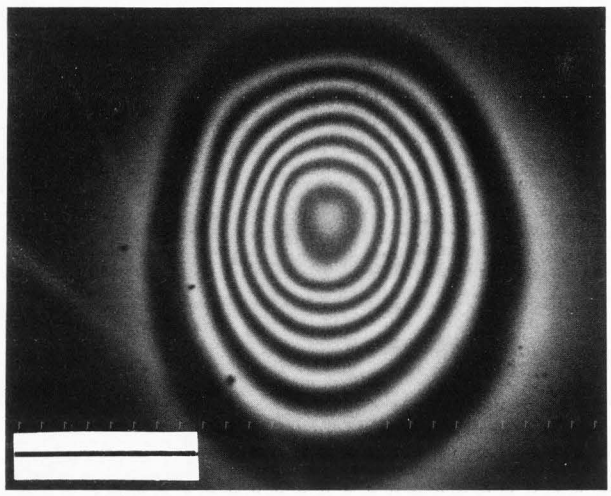

Fig. 3. SEI contour map of a sputter crater formed in a 200 Å Al, 270 Å Al_2O_3 multilayered film. The dark rings are Al, the light rings are Al_2O_3. Bar = 1 mm.

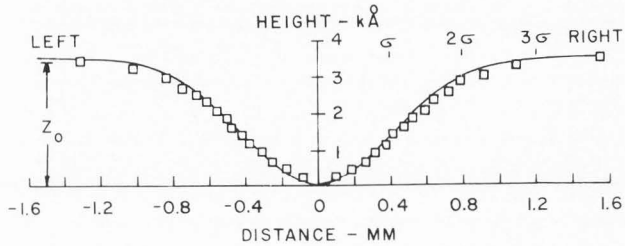

Fig. 4. Cross-section of the contour mapped crater shown in Fig. 3. This cross-section was plotted from the measured distances between the crater center and the edges of successive rings along a horizontal line. Elevations were calculated from the known thicknesses of successive rings. Multiples of the variance σ are shown for a Gaussian curve (solid line) based on Z_o=3500 Å at 3σ.

edge of the contour map in Fig. 7 is typical of the crater shape produced by a static, well collimated beam for the ims 3f. (The shape is considered to depend on the physical geometry of the instrument since it has been observed to be independent of the absence or presence of magnetic fields, or the absence or presence and variation of exterior electric fields.) The detail within the triangular spot demonstrates the complexity of comparing beam density figures obtained at different analysis times or with different instruments.

Discussion

The contour mapping of sputter craters in multilayer films permits the user of the apparatus to examine ion beam sputter characteristics in situ. If the ion beam has a non-Gaussian

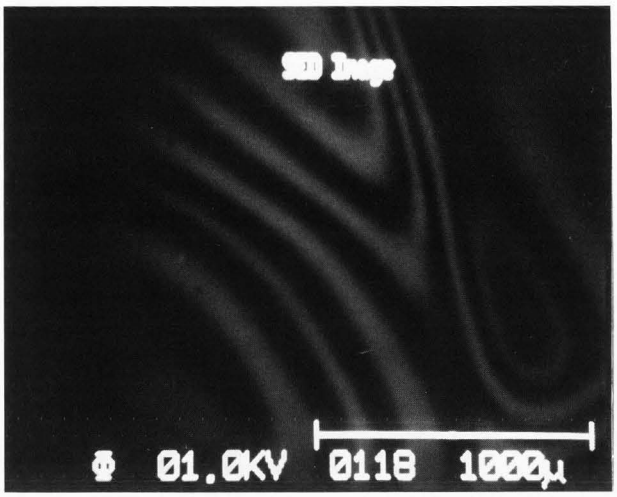

Fig. 5. SEI contour map formed by an Ar^+ beam rastered over 3x3 mm for 72 min. Bar=1000 μm.

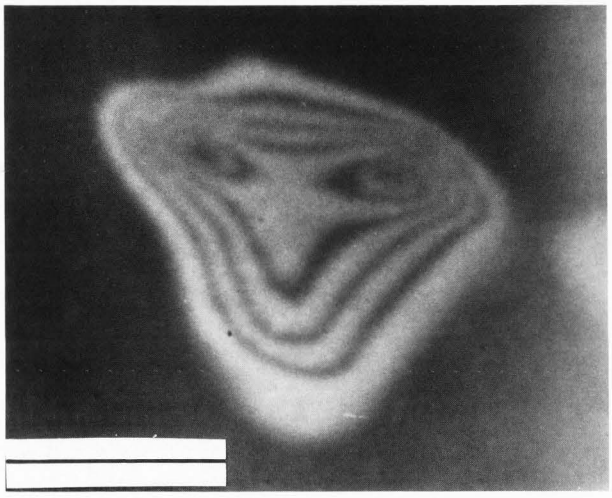

Fig. 7. $^{16}O^-$ ion contour map of a crater formed in a few seconds by a static Cs^+ ion beam. The Cs^+ beam was then rastered over 500 x 500 μm to obtain this image. Bar = 100 μm.

shape, this is easily seen in the contours of the crater it etches. A Gaussian beam at normal incidence to a smooth surface produces a fairly smooth Gaussian crater near the crater center when sputter depths are modest (several thousand Angstroms).

The main criterion for multilayer films in contour mapping of sputter craters is that there be high image contrast between the alternating layers. Al/Al_2O_3 sandwiches were used in this study but other combinations, such as Al/SiO_2, could also be used. In this case, an outer film of SiO_2 would be convenient for locating the impact area of an ion beam because SiO_2 produces a bright secondary electron image during ion bombardment. Also the sputtering yields of Al, Si and O are similar for Ar^+ beams between 500 and

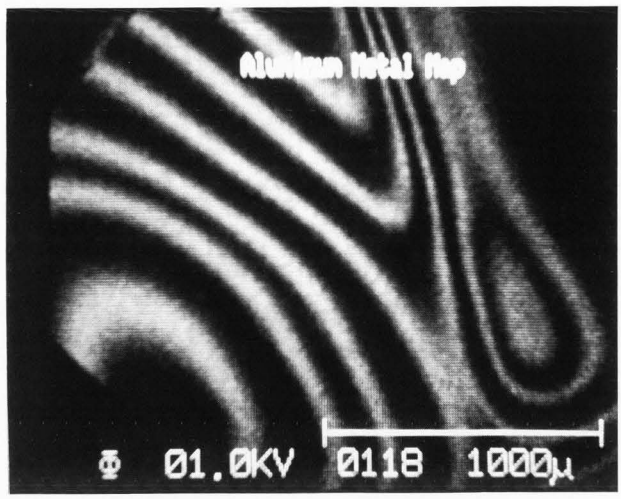

Fig. 6. Al Auger map of the same area as in Fig. 5. Bar = 1000 μm.

1000 eV [11]. There should not be a great difference in sputtering rate of the selected materials. Differential sputtering could produce a distorted crater.

The thicknesses of the alternating layers are arbitrary. However, thicknesses between 200 and 300 Å appear to be useful for most applications of the type described here. The RMS surface roughness of the films must be small compared to their thickness. For the films used here, no surface structure could be observed at magnifications of 10^5 in the PHI Model 595.

Summary

Multilayered films composed of metal, metal oxide couples several hundred Angstroms thick are shown to be useful for the contour mapping of sputter craters. If the ion beam has a Gaussian current density distribution, the crater sputtered by the static beam will have an approximately Gaussian cross-section. In-situ contour mapping allows the operator to adjust a rastered ion beam source so that the crater bottom is nearly flat and the crater center is coincident within the area viewed by the instrument detector.

References

1. Carter, G, Nobes, MJ, Arshak, KI, Webb, RP, Evanson, D, Eghawary, BDL, Williamson, JH (1979). The influence of non-uniform incident flux upon surface erosion processes. J. Mat. Sci. 14, 728-736.

2. Coburn, JW (1979). The influence of ion sputtering on the elemental analysis of solid surfaces. Thin Solid Films 64, 371-382.

3. Davis, LE, MacDonald, NC, Palmberg, PW, Riach, GE, Weber, RE (1976). Handbook of Auger Electron Spectroscopy, Physical Electronics Industries, Eden Prairie, MN, p. 45-47.

4. Hofmann, S, Erlewein, J, Zalar, A (1977). Depth resolution and surface roughness effects in sputter profiling of NiCr multilayer sandwich samples using Auger electron spectroscopy. Thin Solid Films 43, 275-283.

5. Hofmann, S (1980). Quantitative depth profiling in surface analysis: A Review. Surf. Interface Anal. 2, 148-160.

6. Hoffman, DW (1975). A cratering analysis for quantitative depth profiling by ion beam sputtering. Surf. Sci. 50, 29-52.

7. Holloway, PH, Bhattacharya, RS (1981). Limitations of ion etching for interface analysis. Surf. Interface Anal. 3, 118-125.

8. Levenson, LL (1985). Contour mapping of sputter craters with Al/Al_2O_3 multilayered films. J. Vac. Sci. Technol., 3A, 687-688.

9. Malherbe, JB, Sanz, JM, Hofmann, S (1981). Depth resolution factor of a static Gaussian ion beam. Surf. Interface Anal. 3, 235-239.

10. Newbury, DE (1981). Imaging strategy in the scanning electron microscope. Scanning Electron Microsc. 1981; I: 71-78.

11. Seah, MP (1981). Pure element sputtering yields using 500-1000 eV argon ions. Thin Solid Films 81, 279-287.

12. Seah, MP, Hunt, CP (1983). The depth dependence of the depth resolution in composition-depth profiling with Auger electron spectroscopy. Surf. Interface Anal. 5, 33-37.

13. Smith, RW, Walls, JM (1979). The development of surface topography during depth profiling in Auger electron spectroscopy. Surf. Sci. 80, 557-565.

14. Vandervorst, W, Maes, HE, DeKeersmaecker, R (1982). On the influence of crater edges and neutral beam component on impurity profiles from raster scanning SIMS. Surf. Interface Anal. 4, 245-252.

15. Werner, HW (1980). Quantitative secondary ion mass spectrometry: A Review. Surf. Interface Anal. 2, 56-74.

16. Werner, HW (1982). The depth dependence of the depth resolution in sputter profiling. Surf. Interface Anal. 4, 1-7.

17. Wittmaack, K (1977). Raster scanning depth profiling of layer structures. Appl. Phys. 12, 149-156.

18. Zalar, A, Hofmann, S (1980). Crater edge profiling of Ni/Cr sandwich multilayer thin films by scanning Auger microscopy (SAM). Surf. Interface Anal. 2, 183-186.

Discussion with Reviewers

S. Hofmann: Are the different thicknesses of Al (200 Å) and Al_2O_3 (267 Å) chosen to compensate for different sputtering rates? The contour widths of the layers vary by about a factor of two (Figs. 3 and 4). Does this indicate a differing sputtering rate and can the contour map be used to determine such differences?
Authors: The different thicknesses were originally chosen for the study of another phenomenon (plasmon energies in multilayered films). As seen by the eye, the contour widths of the layers in the micrograph (Fig. 3) are subjective because of the high contrast. A composition profile recording the peak intensities of the Al KLL transitions from Al and from Al_2O_3 layers shows that the sputter rates for Al and Al_2O_3 are very nearly equal for the sample used. If the ion beam current density distribution is constant during profiling and reproducible from sample to sample, gross differences in sputtering rates might be detected from contour maps scanned with a microphotometer. However, quantitative measurements of sputtering rate differences probably would be difficult to make.

S. Hofmann: The peculiar feature on the right side of Figs. 5 and 6 suggest an extra spot of high current density. How can this be rationalized in view of the usage of a rastered ion beam?
Authors: The example given in Figs. 5 and 6 is that of a pathological ion beam optical system. Here, the beam shape was not constant as a function of its position on the sample during rastering. The result was a highly distorted contour map, especially near the crater edge.

S. Hofmann: Al_2O_3 is known to decompose by electron beam impact. Is this not a disadvantage particularly if line scans over the crater are performed?
Authors: Al_2O_3 is also expected to decompose under ion beam impact, so that the cratering process by sputtering will affect composition. Moreover, in this study the Al and the Al_2O_3 films were deposited by electron beam evaporation. For the purpose of preparing multilayered samples of the type described, the amount of decomposition by either ion beam or electron beam impact is not sufficient to greatly influence the contrast between layers as seen in SEM, SAM or SIMS.

M. B. Chamberlain: Because the current density in an ion-beam cross section should be periodically measured to ensure long term stability in the sputtering characteristics of a beam, do you think that a reference material, such as your Al/Al_2O_3 laminate should be readily available to surface analysts for comparing results measured both in a single spectrometer at different times as well as in different spectrometers?
Authors: Yes.

M. B. Chamberlain: Sometimes it is impossible to combine profilometry with sputter profiling to measure the thicknesses of each layer in a thin film laminate because the stylus scratches too deeply into the specimen. Have you, or do you think it is practical, to measure the layer thicknesses in a laminate, whose compositions are known but whose layer thicknesses are not, by employing the analysis delineated in Fig. 4? Such an analysis would first establish the depth sputtered into the reference material as a

function of position on the sputtered crater. The second step would be to use these depths, and the sputtering rates appropriate to the layers in the unknown specimen to determine the layer thicknesses in the unknown sample.
Authors: In principle the procedure outlined is possible, but in practice it would be tedious. Other approaches, such as cross-sectioning, angle lapping and ball cratering would probably be easier to apply, according to the composition of the sample and the film thicknesses. For example, see: Levenson, L.L. (1984), Thick coating Analysis with Scanning Auger Electron Spectroscopy, Scanning Electron Microsc. 1984; III: 1211-1218.

Reviewer 2: Can you please comment on your method in relation to a similar method reported many years ago which involves only visual inspection of beam-induced color changes (J.W. Guthrie and R.S. Blewer, Rev. Sci. Instrum. 43 (1972) 654)?
Authors: The visual inspection of beam-induced color changes requires that the sample be inserted and withdrawn from the instrument. The method outlined in the present paper allows the crater to be inspected *in situ* so that changes made in the beam parameters can be visualized in the secondary electron image, etc. In this way, if corrections can be made by changing beam parameters, this can be carried out quickly. Even if internal adjustments must be made, the ease of usage still gives the multifilm sample an advantage.

Reviewer 2: In a given instrument the shape of the beam can equally well or even better be checked by electrical means. The uniformity of the mean current density produced by a raster-scanned beam does not deserve routine control (see ref. 17), provided the respective power supply works properly. Are not Figs. 5 and 6 simply demonstrating the poor quality of the instrument employed by the authors?
Authors: No! In fact, Fig. 3 was made with the same model instrument (PHI 595) but with two instruments at different laboratories. Both instruments were routinely used for sputter profiling, but one sputter gun was not performing as well as the other. This was not obvious from Faraday cup measurements of beam current. The type of pathological conditions shown in Figs. 5 and 6 likely would not be demonstrated with a Faraday cup because such a measurement would be very tedious to carry out.

Reviewer 2: The suggested method does not provide any information about the surface topography and the erosion rate for other sample materials. Therefore, other (external) means for measuring the shape and depth of the crater produced in the analyzed sample are indispensible, e.g. a surface profilometer such as a 'Talysurf' (see ref. 17) or an optical interferometer (H. Liebl, J. Vac. Sci. Technol. 12 (1975) 385).
Authors: Our paper is intended to show how a simple multilayer sample can be used to visualize the shape of a sputter crater so that one can tell if the sputter gun is operating correctly. The method is not intended as a measure of sputter rates.

Reviewer 2: Can you comment on the basic physical problems related to your observations?
Authors: This paper was not intended to address basic problems, only a practical solution to a common problem.